IET Generation, Transmission & Distribution

Research Article

Linear daily UC model to improve the transient stability of power system

ISSN 1751-8687
Received on 15th March 2018
Revised 20th March 2019
Accepted on 23rd April 2019
doi: 10.1049/iet-gtd.2018.5102
www.ietdl.org

Salar Naghdalian[1], Turaj Amraee[1] ✉, Sadegh Kamali[1]
[1]Faculty of Electrical Engineering, K.N. Toosi University of Technology, Tehran, Iran
✉ *E-mail: amraee@kntu.ac.ir*

Abstract: As coherency of generators decreases, the risk of rotor angle instability increases, especially under severe contingencies. The slow coherency as a network characteristic may be controlled by the locations of committed generators. Unit commitment (UC) problem is conventionally carried out regarding operational and network constraints. In this study, a two-step strategy is developed to promote the slow coherency via the network constrained UC (NCUC) model on a daily horizon. First, conventional NCUC is executed. The most important generators with both economic and coherency merits are then determined as representative generators. In the second step, the Slow Coherency Based Unit Commitment (SCBUC) is re-optimisedaccording to the results obtained from the first step, using a multi-objective function. The first part of the multi-objective function is devoted to the cost of generation, start-up, and shutdown of generators. The goal of the second part of the multi-objective function is to maximise the coherency between the committed generators to reach a transient stability margin. The proposed model is converted to a mixed integer linear programming model. The performance of the proposed method of promoting transient stability is investigated using the dynamic IEEE 118-bus test system.

Nomenclature

Sets and subscripts

t	index for time
$i,\ j$	index for bus number
w	index for each segment of linearised function
$\Omega_{\rm b}$	set of all buses
$\Omega_{\rm g}$	set of generator buses
$\Omega_{\rm S}$	set of representative generators
$\Omega_{\rm T}$	set of hours in study horizon
$\Omega_{\rm W}$	set of linearised segments
$\{\cdot\}^{\rm pc}$	subscript for the generation cost
$\{\cdot\}^{\rm sc}$	subscript for the start-up cost
$\{\cdot\}^{\rm sd}$	subscript for the shutdown cost
$\{\cdot\}^{\max}$	maximum value of a given variable
$\{\cdot\}^{\min}$	minimum value of a given variable

Parameters

$a_i,\ b_i,\ c_i$	coefficients of the generation cost function
$C_i^{\rm SUp}$	start-up cost of generator i
$C_i^{{\rm SD}n}$	shutdown cost of generator i
$R_i^{\rm up}$	ramp-up limit of generator i
$R_i^{\rm dn}$	ramp-down limit of generator i
${\rm UT}_i^{\rm on}$	minimum up-time of generator i
${\rm DT}_i^{\rm off}$	minimum down-time of generator i
$P_i^{\max}/P_i^{\min}$	maximum/minimum active power limits of generator i
$Q_i^{\max}/Q_i^{\min}$	maximum/minimum reactive power limits of generator i
${\rm AD}_i^t/{\rm RD}_i^t$	active/reactive demands for bus i at time t
$B_{{\rm w}i}$	power generation at the start of the segment w
$S_{{\rm w}i}$	slope of the segment w in the linearised cost function
G_{ij}/B_{ij}	real/image parts of admittance matrix between bus i and bus j
$R_{\rm SR}^t$	required amount of spinning reserve at time t
$R_i^{\max}$	maximum available reserve related to generator i
${\rm FL}_{ij}$	maximum active flow of transmission line linking bus i and bus j
${\rm SED}_{i,s}^t$	electrical distance between generator i and the representative unit s at time t
H_i	inertia time constant of generator i

Variables

u_i^t	binary variable for on/off statuses of generator i at time t
p_i^t/q_i^t	active/reactive generation of bus i at time t
$v_i^t\angle\theta_i^t$	voltage phasor of bus i at time t
$X_{i,t}^{\rm on}$	number of continuous hours that generator i has been on at time t
$X_{i,t}^{\rm off}$	number of continuous hours that generator i has been off at time t
R_i^t	spinning reserve by generator i at time t ($i\in\Omega_{\rm g}$)
$\lambda_{i{\rm w}}^t$	length of power segment w at time t for cost function of generator i
y_i^t	auxiliary variable for linearising cost function of generator i at time t
$\alpha_i^t,\ \beta_i^t,\ \gamma_i^t$	auxiliary variables for linearising minimum up-time constraints of generator i at time t
$\xi_i^t,\ \eta_i^t,\ \mu_i^t$	auxiliary variables for a linearising minimum down-time constraints of generator i at time t
$k_s(l)$	slope of the lth piecewise linear block of $(\theta_{ij}^t)^2$
$\Delta\theta_{ij}^t(l)$	length of an lth piecewise linear block of θ_{ij}^t
$\theta_{ij}^{t+},\ \theta_{ij}^{t-}$	positive variables as replacement of θ_{ij}^t
ω_i	rotor speed of generator i
$L_{i,s}^t$	auxiliary variable in linearising coherency constraint between generator i and representative unit s at time t
${\rm DV}_{i,s}^t$	binary variable used to specify the electrical distance of generator i from its representative generator

1 Introduction

Unit commitment (UC) is a fundamental problem in power systems optimal scheduling, whose primary goal is to determine the on/off statuses and economic dispatch of generating units in a daily or weekly horizon [1]. The main objective in the UC problem usually is the minimisation of generation cost, start-up cost, and emission cost. This problem encompasses various operational and security constraints. Network constraints are an imperative part of the UC problem [1, 2]. Network constraints mostly focus on the fulfilment of steady-state conditions using AC power flow constraints.

In recent years, by increasing the penetration level of low inertia distributed generation technologies, several models have been proposed to include the transient stability in power system studies. Two approaches are utilised for transient stability enhancement in operational studies such as UC programme. In the first approach, the transient stability is considered using time-domain simulations or transient energy functions in the optimisation model of the power system operation studies. In simulation-based methods, it is required to solve the discretised non-linear swing equations along with the steady-state model of the original network constrained unit constrained (NCUC) model. Also, the digital power system simulators can be utilised to assess the transient stability as well as to determine the critical and non-critical generators using extended equal area criterion (EEAC) method. Also in the energy function method, it is required to define a suitable transient energy function over the system state variables such as speed and rotor angles of generators. Although the first approach methods are valuable; however, due to the computational complexity of discretised swing equation, the efficiency of the transient stability constrained (TSC) NCUC model remains a major problem. In the second approach, the transient stability assessment is not directly included inside the optimisation model of NCUC. Instead, an index is introduced to promote the transient stability of the power system, indirectly. In this regard, the second approach may be interpreted as an alternative for improving the transient stability in the UC study. In this research, the transient stability of the UC problem is improved indirectly using the coherency criterion. The transient stability is improved based on the increasing slow coherency criterion.

Transient stability has been considered in the optimal power flow (OPF) model [3–6]. In TSC-OPF studies, the optimal generation of generating units are determined in such a way that a minimum critical clearing time (CCT) is preserved without considering the on/off statuses of generating units. In [7], a decomposition-based approach has been developed to consider the transient stability in security constrained UC model using EEAC. Also, the digital power system simulator has been utilised to identify the critical and non-critical generators. Similar work has been done in [7]. In [8], an augmented Lagrange relaxation method has been utilised to solve the TSC-OPF as a sub-problem of the UC programme. Also in [8], a reduced space interior point method has been utilised to solve the TSC-OPF sub-problem directly. In recent years, the integration of renewable energy resources such as wind power has created more complexities in UC models of modern power systems [9]. In [10–12], frequency stability constraints have been proposed to fulfil the safety of system frequency response. In previous proposed TSC UC models, the transient stability assessment is done directly using the swing equation with some simplification using EEAC method or a digital power system simulator. Less effort has been done to improve the transient stability of Security Constrained Unit Commitment model indirectly.

Slow coherency between synchronous generators is a physical confirmation of a weak connection. As coherency of generators increases, the risk of rotor angle instability in power system decreases [13]. The coherency between synchronous generators depends on the network characteristics as well as the relative locations of generators. Therefore, the coherency of generators is affected by the unit scheduling and their dispatch. In [14], it has been shown that the grid structure especially the electrical distances among the generator internal buses has a great impact on power system dynamics.

In a power system, the generators with similar dynamic responses are called coherent units [15]. In addition to enhancing transient stability margin [13, 15], increasing the coherency of generators has a great effect on mitigating low-frequency power swings, especially in islanding conditions [16]. In previous studies, no effort has been done to promote the slow coherency via the daily unit scheduling.

In the literature, several approaches including model-based and measurement-based methods have been presented to discern the coherency of generators [13]. The model-based methods mainly rely on modal analysis. Hence, they are not suitable for the UC problem, due to the high computational burden. Since UC is an off-line task, the measurement-based methods are not applicable to the UC problem too. In [14], it has been shown that the electrical distance between generators has a great impact on dynamic interactions between generators.

In this paper, a two-step strategy is developed to improve the slow coherency of synchronous generators in daily scheduling of generating units. In the first step, the conventional NCUC model is solved. The coherency of committed generators is then determined using a coherency index. According to the obtained coherency and economic merits, for each area, a generator is selected as the representative generator of that area. In the second step, the Slow Coherency Based Unit Commitment (SCBUC) is optimised while the coherency is integrated inside the NCUC using the electrical distance criterion. An iterative-based process is considered to determine the weighting factors until providing target minimum CCT. The desired minimum CCT is considered as the stopping criterion for coherency improvement. To promote the computational efficiency of the proposed method, the SCBUC along with the AC power balance constraints are linearised and solved using CPLEX algorithm. The main contributions of this paper are two-fold:

- Developing an analytic framework to promote the slow coherency of the network via a two-step SCBUC model.
- Providing the transient stability margin indirectly using the coherency concept.
- Providing an iterative-based approach for adjusting weighting factors of the proposed multi-objective function to reach the target minimum CCT.
- Developing a mixed integer linear programming (MILP) model for the proposed SCBUC model to assure the optimality of the obtained schedule.

Regarding the flowchart shown in Fig. 1, the structure of the proposed two-step strategy is described. The first step of the proposed strategy contains some subsequent stages as follows:

- Executing the MILP model of NCUC programme without considering the coherency constraint, as described in Section 2 and using (5) and (7)–(32).
- Determining the representative generator in each region as described in Section 3.1, using (33) and (34).
- Constructing the electrical distance matrix using data obtained from the NCUC model as described in Section 3.2, formulated in (35) and (36).

The second step of the proposed strategy acts based on some useful information obtained from the first step as follows:

- Constructing the objective functions of the proposed SCBUC including the operational cost of generators and coherency-based objective function as described in Sections 3.3 and 4, using (37)–(44).
- Optimising the multi-objective MILP-based SCBUC model and doing time-domain simulations.
- Adjusting the ratio of weighting factors [i.e. (ρ_1/ρ_2)] in an iterative-based process as described in Section 4, to achieve the target minimum CCT.

The goal of the first step of the proposed strategy is determining the representative generators using the results obtained from conventional NCUC model, and finally constructing the electrical distance matrix. The goal of the second step of the strategy is to formulate the multi-objective SCBUC including the operational cost and coherency of generators and adjusting weighting factors to

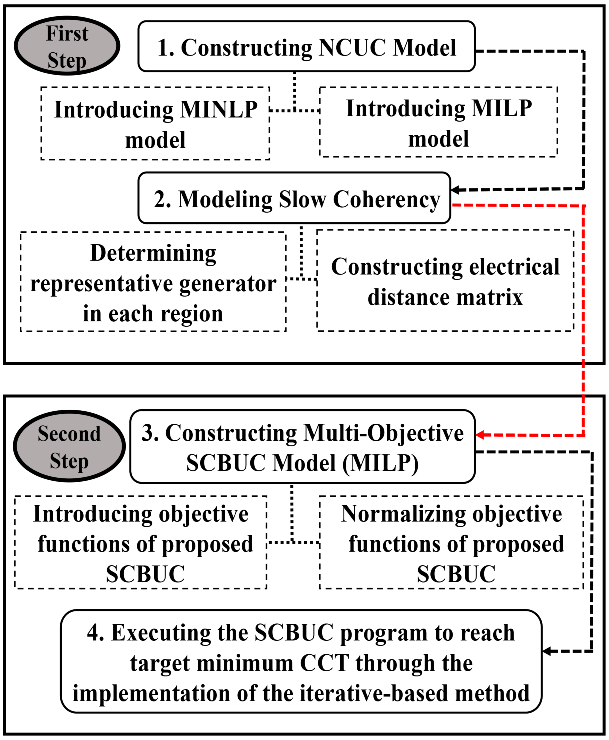

Fig. 1 *Flowchart of the proposed two-step strategy*

reach the target minimum CCT based on an iterative process. The rest of this paper is organised as follows. In Section 2, the non-linear and linear formulations of the NCUC model is presented. In Section 3, the formulation of the slow coherency criterion as the most notable innovation of this work is described. In Section 4, the multi-objective function of the proposed SCBUC is presented and the iterative-based process to reach the target minimum CCT is introduced. The simulation results on a modified IEEE 118-bus test system are presented in Section 5. Finally, this paper is concluded in Section 6.

2 Linear formulation of the NCUC problem

The non-linear forms of the objective function and the operational constraints of units could be found in [1]. Network constraints including load flow [i.e. (1) and(2)], bus voltage limits and line flow limits [i.e. (3) and (4)] are applied for each bus $i \in \Omega_b$ at each time $t \in \Omega_T$. In load flow equations [i.e. (1) and (2)], the variables p_i^t, q_i^t are fixed to zero in load buses. The reserve requirement [i.e. (5)] is defined for the entire network and each unit

$$p_i^t u_i^t - \mathrm{AD}_i^t = \sum_{j \in \Omega_b} V_i^t V_j^t \left(G_{ij}\cos\left(\theta_{ij}^t\right) + B_{ij}\sin\left(\theta_{ij}^t\right)\right) \tag{1}$$

$$q_i^t u_i^t - \mathrm{RD}_i^t = \sum_{j \in \Omega_b} V_i^t V_j^t \left(G_{ij}\sin\left(\theta_{ij}^t\right) - B_{ij}\cos\left(\theta_{ij}^t\right)\right) \tag{2}$$

$$V_{i,t}^{\min} \le V_i^t \le V_{i,t}^{\max} \tag{3}$$

$$-\mathrm{FL}_{ij} \le (V_i^t)^2 G_{ij} - V_i^t V_j^t G_{ij}\cos\left(\theta_{ij}^t\right) - V_i^t V_j^t B_{ij}\sin\left(\theta_{ij}^t\right) \le \mathrm{FL}_{ij} \tag{4}$$

$$\sum_{i \in G} R_i^t \ge R_{\mathrm{SR}}^t,\ R_i^t \le P_i^{\max} u_i^t - P_i^t,\ \ R_i^t \le R_i^{\max} \tag{5}$$

The thermal limit of a given transmission line can be expressed based on the maximum ampere capacity or maximum active power. Since in this paper, the power flow model has been expressed based on the standard active and reactive power formulations, the thermal limits of transmission lines are expressed based on the maximum allowable active flow. Additionally, the thermal limits of transmission lines in most of IEEE benchmark test grids such as IEEE 118-bus test system are available based on the maximum active power flow limits.

2.1 Objective function

The objective function of the NCUC problem conventionally includes the generation cost, start-up cost, and shutdown cost of units over a daily horizon. This objective function is linearised using (6)–(14). The auxiliary binary variable $\boldsymbol{y}_i^t = \boldsymbol{u}_i^t \boldsymbol{u}_i^{t-1}$ is defined for linearising the cost function. The expression given in (6) refers to the generation cost of thermal units at the minimum allowed power generation. For each generator, the limit of active power is segmented by (7). The slope of each segment in the utilised piecewise linearising method is determined by (8). The length of each power segment is limited by (9). There are various approaches to linearise the start-up and shutdown costs [17, 18]. Here, the start-up and shutdown costs are linearised by (13) and (14), respectively

$$f^{\mathrm{pc}}\left(P_i^{\min}\right) = C_i P_i^{\min 2} + b_i P_i^{\min} + a_i, \quad \forall i \in \Omega_{\mathrm{g}} \tag{6}$$

$$B_{wi} = p_i^{\min} + (p_i^{\max} - p_i^{\min})\frac{w}{N}, \quad \forall w \in \Omega_{\mathrm{W}},\ \forall i \in \Omega_{\mathrm{g}} \tag{7}$$

$$S_{wi} = \frac{\left[f^{\mathrm{pc}}(\tau_{wi}) - f^{\mathrm{pc}}\left(\tau_{(w-1)i}\right)\right]}{B_{wi} - B_{(w-1)i}},\ B_{0i} = p_i^{\min}, \quad \forall w \in \Omega_{\mathrm{W}},\ \forall i \in \Omega_{\mathrm{g}} \tag{8}$$

$$0 \le \lambda_{iw}^t \le (B_{wi} - B_{(w-1)i})u_i^t,\ \forall w \in \Omega_{\mathrm{W}},\ \forall i \in \Omega_{\mathrm{g}},\ \forall t \in \Omega_{\mathrm{T}} \tag{9}$$

$$f^{\mathrm{pc}}\left(p_t^i\right) = u_i^t p_i^{\min} + \sum_{w \in N} S_{wi}\lambda_{iw}^t, \quad \forall i \in \Omega_{\mathrm{g}},\ \forall t \in \Omega_{\mathrm{T}} \tag{10}$$

$$-(1 - u_i^{t-1}) \le u_i^t - y_i^t \le (1 - u_i^{t-1}), \quad \forall i \in \Omega_g,\ \forall t \in \Omega_T \tag{11}$$

$$0 \le y_i^t \le u_i^{t-1}, \quad \forall i \in \Omega_{\mathrm{g}}, \quad \forall t \in \Omega_{\mathrm{T}} \tag{12}$$

$$f^{\mathrm{sc}}(u_i^t) = (u_i^t - y_i^t)C_i^{\mathrm{SU_P}}, \quad \forall i \in \Omega_{\mathrm{g}}, \quad \forall t \in \Omega_{\mathrm{T}} \tag{13}$$

$$f^{\mathrm{sd}}\left(u_t^i\right) = (u_i^{t-1} - y_i^t)C_i^{\mathrm{SD}_n}, \quad \forall i \in \Omega_{\mathrm{g}},\ \forall t \in \Omega_{\mathrm{T}} \tag{14}$$

2.2 Operational constraints

2.2.1 Ramping constraints: The non-linear forms of the ramping-up and ramping-down constraints are discussed in [1]. Using the auxiliary binary variable y_i^t, the linear form of ramping constraints are expressed as given in (15) and (16) for each unit $i \in \Omega_{\mathrm{g}}$ at each time $t \in \Omega_{\mathrm{T}}$, respectively

$$p_i^t - p_i^{t-1} \le (1 - u_i^t + y_i^t)R_i^{U_\mathrm{P}} + (u_i^t - y_i^t)P_i^{\min} \tag{15}$$

$$p_i^{t-1} - p_i^t \le (1 - u_i^{t-1} + y_i^t)R_i^{D_n} + (u_i^{t-1} - y_i^t)P_i^{\min} \tag{16}$$

2.2.2 Power production limits: The active and reactive power generations of each generator is limited by its physical characteristics, which are given by the manufacturer. These constraints are formulised by the equations below:

$$P_i^{\min} u_i^t \le p_i^t \le P_i^{\max} u_i^t, \quad \forall i \in \Omega_{\mathrm{g}}, \quad \forall t \in \Omega_{\mathrm{T}} \tag{17}$$

$$Q_i^{\min} u_i^t \le q_i^t \le Q_i^{\max} u_i^t \quad \forall i \in \Omega_g,\ \forall t \in \Omega_T \tag{18}$$

2.2.3 Minimum up-time limit: Owing to technical reasons, each generator must be on/off for a specific number of hours after a start/shutdown action. The auxiliary variables $\beta_i^t = X_{i,t-1}^{\mathrm{on}} u_i^{t-1}$, $\alpha_i^t = X_{i,t-1}^{\mathrm{on}} u_i^t$, and $\gamma_i^t = X_{i,t-1}^{\mathrm{on}} y_i^t$ are, respectively, linearised by (19), (20); (21), (22); and (24), (25). The minimum up-time equations then linearised using (23) and (26), for each unit $i \in \Omega_g$ at each time $t \in \Omega_T$, respectively

$$-(1-u_i^{t-1})M \le X_{i,t-1}^{\text{on}} - \beta_i^t \le (1-u_i^{t-1})M \quad (19)$$

$$0 \le \beta_i^t \le u_i^{t-1}M \quad (20)$$

$$-(1-u_i^t)M \le X_{i,t-1}^{\text{on}} - \alpha_i^t \le (1-u_i^t)M \quad (21)$$

$$0 \le \alpha_i^t \le u_i^t M \quad (22)$$

$$\beta_i^t - \text{UT}_i^{\text{on}} u_i^{t-1} - \alpha_i^t + \text{UT}_i^{\text{on}} u_i^t \ge 0 \quad (23)$$

$$-(1-y_i^t)M \le X_{i,t-1}^{\text{on}} - \gamma_i^t \le (1-y_i^t)M \quad (24)$$

$$0 \le \gamma_i^t \le y_i^t M \quad (25)$$

$$X_{i,t}^{\text{on}} = u_i^t + \gamma_i^t \quad (26)$$

2.2.4 Minimum down-time limit: To linearise the minimum down-time constraints, the auxiliary variables $\xi_i^t = X_{i,t-1}^{\text{off}} u_i^{t-1}$, $\eta_i^t = X_{i,t-1}^{\text{off}} u_i^t$, and $\mu_i^t = X_{i,t-1}^{\text{off}} y_i^t$ are utilised and the process of linearisation of minimum down-time equations is the same as minimum up-time equations. The minimum down-time constraints then linearised using (27) and (28), for each unit $i \in \Omega_g$ at each time $\in \Omega_T$, respectively

$$\eta_i^t - \text{DT}_i^{\text{off}} u_i^t - \xi_i^t + \text{DT}_i^{\text{off}} u_i^{t-1} \ge 0 \quad (27)$$

$$X_{i,t}^{\text{off}} = 1 + X_{i,t-1}^{\text{off}} - \xi_i^t - u_i^t - \eta_i^t + \mu_i^t \quad (28)$$

2.3 Linearising AC power flow equations

A combinatorial techniques relying on Taylor series expansion and utilising binary variables are utilised to linearise the AC power flow equations. The non-linear terms of power flow equations given by (1) and (2) are replaced by the simplified approximation relying on Taylor series expansion as given in Table 1. It is noted that the approximations are determined at the normal operational point (i.e. $V_i^t = 1$, $V_j^t = 1$, $\theta_{ij}^t = 0$). The linearising technique including auxiliary binary variables, as discussed in [19], is employed to linearise the term θ_{ij}^{t2}. According to the constraints given in (17) and (18), the linearised form of the AC load flow equations can be formulised as follows:

$$\begin{aligned} p_i^t - \text{AD}_i^t = (2V_i^t - 1)G_{ii} + \sum_{j \in \Omega_g \,\&\, j \ne i} G_{ij}(V_i^t + V_j^t \\ -\frac{1}{2}\sum_{l \in L} k_s(l)\Delta\theta_{ij}^t(l) - 1) + B_{ij}\theta_{ij}^t \end{aligned} \quad (29)$$

$$\begin{aligned} q_i^t - \text{RD}_i^t = -(2V_i^t - 1)B_{ii} - \sum_{j \in \Omega_g \,\&\, j \ne i} G_{ij}\theta_{ij}^t - B_{ij}\Big(V_i^t + V_j^t \\ -\frac{1}{2}\sum_{l \in L} k_s(l)\Delta\theta_{ij}^t(l) - 1\Big) \end{aligned} \quad (30)$$

Table 1 Taylor expansion of non-linear terms in power flow equations

Non-linear function	Taylor expansion formulation	Simplified formulation
$V_i^t V_j^t \cos(\theta_{ij}^t)$	$V_i^t + V_j^t + \cos(\theta_{ij}^t) - 2$	$V_i^t + V_j^t - \frac{\theta_{ij}^{t\,2}}{2} - 1$
$V_i^t V_j^t \sin(\theta_{ij}^t)$	$\sin(\theta_{ij}^t)$	θ_{ij}^t
$(V_i^t)^2$	$2V_i^t - 1$	$2V_i^t - 1$

where $\theta_{ij}^t = \theta_{ij}^{t+} - \theta_{ij}^{t-}$ and $\sum_{l \in L} \Delta\theta_{ij}^t(l) = \theta_{ij}^{t+} + \theta_{ij}^{t-}$. The slope of each segment is determined by the equation below:

$$k_s(l) = (2\,l - 1)\,\frac{\theta_{ij}^{\max}}{L} \quad (31)$$

Accordingly, the non-linear expression of active line flow given in (4) is linearised for each line from bus i to bus j as given in the equation below:

$$\begin{aligned} -\text{FL}_{ij} \le (2V_i^t - 1)G_{ij} - G_{ij}\Big(V_i^t + V_j^t - \frac{1}{2}\sum_{l \in L} k_s(l)\Delta\theta_{ij}^t(l) - 1\Big) \\ -B_{ij}(\theta_{ij}^t) \le \text{FL}_{ij} \end{aligned} \quad (32)$$

3 Coherency evaluation index

The aim of modelling presented in this section is to extract the criterion which can be used to increase the coherency between generators and improve the transient stability margin indirectly. The electrical distance between the internal nodes of generators has a great impact on their dynamic interactions and coherency [14]. Also in [20, 21], the electrical distance between generators has been considered as a measure of their coherency. The main purpose of the proposed SCBUC model is to increase the coherency of synchronous machines to reach a minimum CCT as the transient stability margin. Coherency is measured between each pair of generators. In this paper, the coherency of each generator is measured with respect to the centre-of-inertia (COI) reference. In this regard, the generator with the highest coherency with the COI reference is selected as the representative generator. The SCBUC problem is solved in such a way that the electrical distance between the committed units and the representative unit in each region is minimised. The coherency constraint is considered in SCBUC model based on the procedure given in Sections 3.1–3.3.

3.1 Determining representative generator in each region

For modelling the slow coherency in NCUC problem using the electrical distance reduction method, representative generators should be considered to measure the electrical distance in each area. Therefore, representative generators are determined as a reference to measure the electrical distance in each area. The representative generators have two important features. First, they have economical merits (e.g. committed in all times based on the conventional NCUC). Second, they have a maximum rotor speed correlation with COI rotor speed of their specified coherent area. Indeed, representative generators are generators with high inertia so the impact of minor changes of network topology in the process of selecting these representative generators is not significant and representative generators are selected with a reasonable approximation.

The boundary of each region is selected based on the slow coherency technique proposed in [16]. Now, for each region, a representative generator is determined as follows:

- Executing the conventional NCUC programme, without considering the coherency constraint.
- Calculating the speed of the COI using (31)

$$\omega_{\text{COI}} = \frac{\sum_{i=1}^{n} H_i\omega_i}{\sum_{i=1}^{n} H_i} \quad (33)$$

- Calculating the correlation between the speed of committed generators (e.g. generators i) and the speed of the COI in each region using the equation below:

$$\text{CR}_{i(\text{COI})} = \frac{n\sum_{t=1}^{n}[\omega_i(t)\omega_{\text{COI}}(t)] - \sum_{t=1}^{n}[\omega_i(t)] \times \sum_{t=1}^{n}[\omega_{\text{COI}}(t)]}{\sqrt{A \times B}} \quad (34)$$

$$A = n\sum_{t=1}^{n}(\omega_i(t))^2 - \left(\sum_{t=1}^{n}\omega_i(t)\right)^2$$

$$B = n\sum_{t=1}^{n}(\omega_{\rm COI}(t))^2 - \left(\sum_{t=1}^{n}\omega_{\rm COI}(t)\right)^2$$

- Selecting the generators with maximum correlation coefficient and economic priority (i.e. committed in all times using conventional NCUC), as the representative generator in each group.

3.2 Constructing electrical distance matrix

To calculate the electrical distance between generating units and the representative generator, the modified $\boldsymbol{Z}$**bus** (i.e. $\mathbf{Zmod}_{ij}^{t}$) including load model and synchronous reactance of generators is now constructed. The reactances of the generators and their step-up transformers are added to the relevant array in $\boldsymbol{Z}$**bus** matrix. The modified $\boldsymbol{Z}$**bus** is calculated according to the equation below:

$$\mathrm{Zmod}_{i,s}^{t} = Z_{i,s}^{t} + \left(X_{\rm d}^{i} + X_{\rm Tr}^{i}\right) + (X_{\rm d}^{s} + X_{\rm Tr}^{s}) \tag{35}$$

The electrical distance between a given unit i and the representative unit s is considered as the coherency index

$$\mathrm{SED}_{i,s}^{t} = \left|\mathrm{Zmod}_{i,s}^{t}\right| \tag{36}$$

3.3 Objective function of slow coherency

The aim of the proposed objective function is to minimise the operational cost and electrical distance (i.e. maximising coherency to enhance transient stability) simultaneously. In the following, the coherency constraints are formulated based on the electrical distance matrix.

The coherency constraints are presented in (37)–(40). The total cost of coherency (i.e. the electrical distance) of the committed generators can be calculated by (41). According to the constraints given in (37)–(40), if a generator is online, its electrical distance from the related representative generator should be computed. Otherwise, it should not be included in the objective function

$$\mathrm{DV}_{i,s}^{t} - 1 \le u_i^t - L_{i,s}^{t} \le 1 - \mathrm{DV}_{i,s}^{t}, \quad \forall i \in \Omega_{\rm g},\ \forall t \in \Omega_{\rm T},\ \forall s \in \Omega_{\rm S} \tag{37}$$

$$0 \le L_{i,s}^{t} \le \mathrm{DV}_{i,s}^{t} \quad \forall i \in \Omega_{\rm g},\ \forall t \in \Omega_{\rm T},\ \forall s \in \Omega_{\rm S} \tag{38}$$

$$\sum_{s \in \Omega_S} \mathrm{DV}_{i,s}^{t} = 1, \quad \forall i \in \Omega_{\rm g},\ \forall t \in \Omega_{\rm T} \tag{39}$$

$$\mathrm{CED}_{i,s}^{t} = L_{i,s}^{t}\mathrm{SED}_{i,s}^{t}, \quad \forall i \in \Omega_{\rm g},\ \forall t \in \Omega_{\rm T},\ \forall s \in \Omega_{\rm S} \tag{40}$$

$$\mathrm{CCF} = \sum_{t \in \Omega_{\rm T}}\sum_{i \in \Omega_{\rm g}}\sum_{s \in \Omega_{\rm S}} \mathrm{CED}_{i,s}^{t}, \quad \forall i \in \Omega_{\rm g},\ \forall t \in \Omega_{\rm T},\ \forall s \in \Omega_{\rm S} \tag{41}$$

4 Multi-objective MILP-based SCBUC model

The weighted summation of the normalised values of both objectives is introduced as the objective function [22]. The two objectives are normalised by (42), in which the operational cost (i.e. F_1) and the cost of coherency (i.e. F_2) are expressed as given by (43) and (44)

$$Z = \sum_{i=1}^{2}\rho_i \frac{F_i(x) - F_i^{\min}}{F_i^{\max} - F_i^{\min}} \tag{42}$$

$$\begin{aligned} F_1 = &\sum_{t \in \Omega_{\rm T}}\sum_{i \in \Omega_{\rm g}}(u_i^t p_i^{\min} + \sum_{w \in \Omega_{\rm W}} S_{wi}\lambda_{iw}^{t}) \\ &+ \sum_{t \in \Omega_{\rm T}}\sum_{i \in \Omega_{\rm g}}(u_i^t - y_i^t)C_i^{\mathrm{SU_P}} + \sum_{t \in \Omega_{\rm T}}\sum_{i \in \Omega_{\rm g}}(u_i^{t-1} - y_i^t)C_i^{\mathrm{SD}_n} \end{aligned} \tag{43}$$

$$F_2 = \sum_{t \in \Omega_{\rm T}}\sum_{i \in \Omega_{\rm g}}\sum_{s \in \Omega_{\rm S}} \mathrm{CED}_{i,s}^{t} \tag{44}$$

Each normalised objective in (42) has a value between 0 and 1. Hence, by tuning the weighting factors ρ_i, the sets of solutions can be obtained. Also by increasing the weighting factor of F_2, the generation cost of NCUC is increased. However, the network operator may have to pay a given additional cost to promote the coherency based on his/her experiences. Practically, the minimum CCT is determined by the operator due to the requirements of the network protection system. The minimum CCT highly depends on the delays of protective relays, circuit breakers. In this scheme, weighting factors should be set using a suitable procedure to achieve the target minimum CCT. Therefore, in order to improve the transient stability margin using minimum CCT criterion the ratio of weighting factors [i.e. (ρ_1/ρ_2)] should be adjusted (i.e. reduced) in favour of the coherency-based part of the multi-objective function.

The solution process of the proposed SCBUC is as follows:

- Optimising SCBUC problem, with $(\rho_1, \rho_2) = (1, 0)$, as given in (42) to compute $F_1^{\min}$ and $F_1^{\max}$.
- Optimising SCBUC problem with $(\rho_1, \rho_2) = (0, 1)$, as given in (42) to compute $F_2^{\min}$ and $F_2^{\max}$.
- Constructing and optimising the SCBUC with new multi-objective function as given in (42) with given weights.
- The ratio of weighting factors is reduced in an iterative-based process as described in Fig. 2 to provide the target minimum CCT.

As shown in Fig. 2, the multi-objective MILP-based SCBUC model is optimised through an iterative-based process. In the

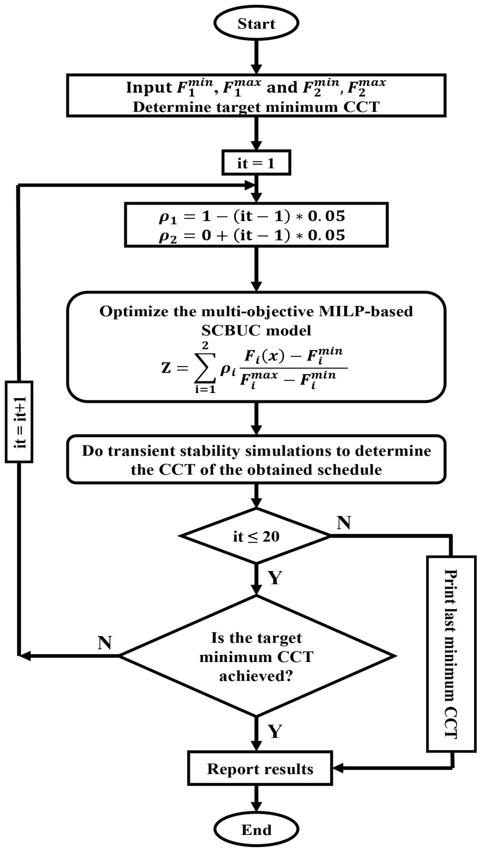

Fig. 2 *Iterative-based process to determine weighting factors*

iterative-based process, the weighting factor of F_1 decreases and the weighting factor of F_2 increases in steps of 0.05. This sort of change will magnify the importance of coherency-based objective function in the proposed multi-objective function. The iterative process continues until the target minimum CCT is reached.

5 Simulation results

In this section, the proposed MILP-based SCBUC model is simulated on a modified IEEE 118-bus test system, as shown in Fig. 3. This system consists of 54 generators and 90 load points. The operational and dynamic data of this system can be found in [23, 24], respectively. The required spinning reserve in each hour is assumed to be 20% of the total system load in that hour (i.e. $\sum_{i\in G} R_i^t = 0.2\sum_{i\in G}\mathrm{AD}_i^t$). The maximum available spinning reserve of each unit is assumed as 20% of its maximum output power. The simulations are carried out in two distinct cases. In case of A, the NCUC model is solved and the results are obtained. In case of B, the SCBUC model is solved, in which the schedule obtained by the NCUC model is utilised to determine the representative generators using time-domain simulations in DIGSILENT. The correlation between generators' speeds, as given by (34), is employed to evaluate the improvement in the coherency of generators. The stopping criterion for determining weighting factors is to reach the CCT of 100 ms. The optimisation models are solved using CPLEX in GAMS [25]. The simulations are performed using a PC with Intel core i7, 4.2 GHz 7700 CPU and 32 GB RAM DDR4. Since the NCUC model has been linearised, a feasible and optimal solution is obtained using the CPLEX algorithm. As the proposed Mixed Integer Programming (MIP) formulation is an approximation of the original MINLP problem, it is noted that cannot be interpreted as the optimal solution of the original MINLP problem. Although we have utilised the approximated linear AC power flow model, the MIP model of NCUC has much lower complexities with respect to the optimal solution of the approximated MILP formulation the MINLP models of NCUC. The relative gap of CPLEX algorithm, which indicates the duality gap is adjusted to zero in all simulation cases.

5.1 NCUC model

In this case, the NCUC problem without considering coherency constraint is solved. Actually, in this case, the weighting coefficients are considered as $\rho_1 = 1$ and $\rho_2 = 0$; hence, operational cost (i.e. F_1) is optimised and the cost of coherency (i.e. F_2) is just calculated. The obtained results including an hourly schedule of units, hourly power production, and reserve are presented in Fig. 4. Now, the obtained commitment schedule is utilised to determine the representative generators using the coherency index. Furthermore, the electrical distance matrix is then utilised as the input of SCBUC.

5.1.1 Determining the representative generators: The commitment schedule obtained using the NCUC model is now analysed by DIGSILENT to determine the representative generator of each group. Although the slow coherency of generators does not vary significantly by the change of initial condition and disturbance [12], here, a 0.2 s three-phase short-circuit fault is applied on all network branches in two operating points, i.e. high demand T12 and low demand T5, to evaluate the coherency of generators. According to the correlation index and the economic merits of generators, the representative generators of all three regions are selected. According to Fig. 4, the generators that are online in all times have economic priority and may be considered as the candidate units. Hence, G10, G12, G25, G26, and G113 in the first group, G49, G65, G66, G70, G76, and G77 in the second group, and G80, G89, G92, and G100 in the third group are considered as the candidate units. The average coherency between these generators and COI for various faults and in hours T5 and T12 is determined. Table 2 presents an example of these calculations. For instance, the units G12, G66, and G92 are chosen as the selected generators in first, second, and third groups, respectively, in hours

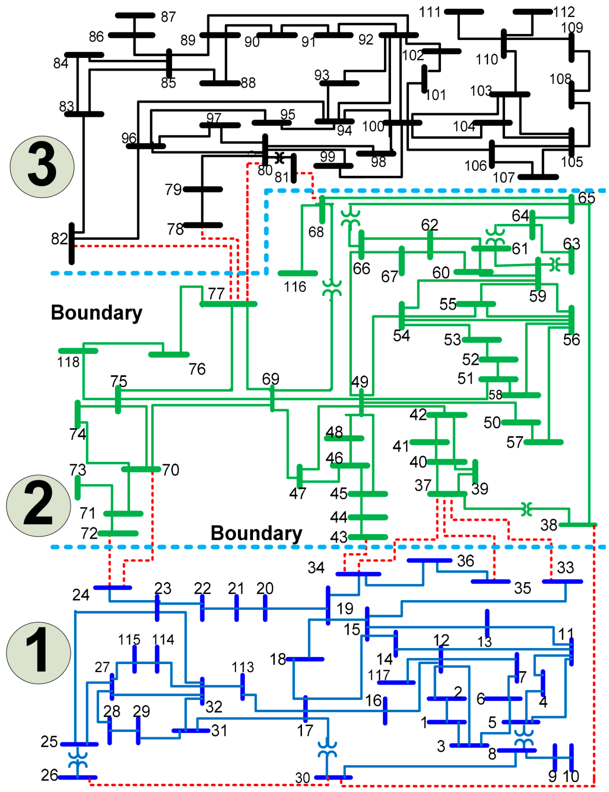

Fig. 3 *Single-line diagram of the IEEE 118-bus system*

T5 and T12 (i.e. $\Omega_S = \{G12,\ G66,\ G92\ \}$). Similarly, this analysis is carried out for all 24 h.

5.1.2 MILP-based SCBUC model: Now, the electrical distance matrix is constructed. The set of representative generators and the electrical distance matrix are passed to the SCBUC model. After determining the representative generators in each group, the SCBUC model incorporates the slow coherency of generators in the UC problem. In this case, the multi-objective model including coherency constraint is solved. The SCBUC problem is first solved with only one objective function (i.e. F1 or F2) and the values of $F_1^{\min}(p_i^t,\ u_i^t,\ y_i^t) = 861,\ 701.150(\$)$ and $F_2^{\min}(\mathrm{DV}_{i,s}^t,\ u_i^t) = 261.4023$, pu are obtained. Similarly, the programme is executed to individually maximise each objective and the values (i.e. daily values) of $F_1^{\max}(p_i^t,\ u_i^t,\ y_i^t) = 2,\ 217,\ 674.3087,\ \$$ and $F_2^{\max}(DV_{i,s}^t,\ u_i^t) = 1081.437$ pu are obtained. The proposed SCBUC model is solved and the ratio of weighting factors [i.e. (ρ_1/ρ_2)] is reduced in an iterative-based process as shown in Fig. 2. The obtained normalised objective costs are presented in Table 3, for different pairs of weighting coefficients. The NCF1 and NCF2 are the normalised values of objective functions F_1 and F_2, respectively $[\mathrm{NCF}_i = (F_i(x) - F_i^{\min})/(F_i^{\max} - F_i^{\min})]$. The desired amount of minimum CCT is practically considered to be between 100 and 200 ms. In this work, the minimum CCT is considered to be equal to 100 ms [26]. According to the simulation results given in the next part, after 11 iterations the weighting coefficients as $\rho_1 = \rho_2 = 0.5$ provides a minimum CCT of 100 ms. The new commitment schedule of generating units, considering the coherency constraint, is presented in Fig. 4, where the differences compared with the first case are highlighted. The simulation results are given in Tables 4 and 5.

The total daily operational and coherency costs of NCUC and SCBUC models are given in Table 4. Also, the hourly operational and coherency cost using NCUC and SCBUC models are reported in Table 5. According to Table 4, using the SCBUC, the total operational cost (i.e. F_1) is increased by 2.328% and the coherency cost (i.e. $F2$) is decreased by 28.162%. It means that the system operator will pay an additional cost (i.e. 881, 765.165–861, and

701.150) to promote the coherency to provide a minimum CCT of 100 ms. Indeed by considering the stopping criterion of CCT = 100 ms, the major challenge in SCBUC to quantise slow coherency index is removed. The modified electrical distance matrix is reported for some hours in Table 6. According to Table 6, in low demand hour T5, the units G70, G76, G77, and G113 are de-committed due to their long electrical distance from the representative generator. Also, the units G82, G111, and G116 have been on, due to their short electrical distance from the representative generators. For numerical verification, in high demand hour T12 a three-phase short-circuit fault is applied in line 30–38, and the rotor speeds of the committed generators in both NCUC and SCBUC models are depicted in Fig. 5. According to Fig. 5, the coherency of generators in Group1 is slightly improved. This improvement is more significant in Group2, where the average coherency index is increased from 0.84285 to 0.9646. This improvement is the result of replacing units G76, G77, G46, and G55 (with, respectively, 0.473775, 0.47375, 0.55512, and 0.5425 pu. electrical distance) by units G31, G40, and G42 (with, respectively, 0.26942, 0.2286, and 0.22617 pu. electrical distance). Similarly, the coherency of units in the third group is considerably improved, where the average coherency index is increased from

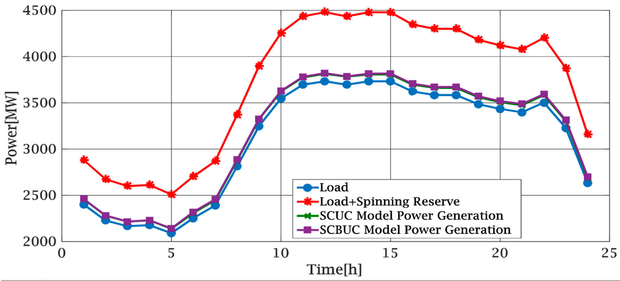

Unit	Hour(h)																						
	1	2	3	4	5	6	7	8	9	10	11	12	13	14	15	16	17	18	19	20	21	22	23	24
G004	0	0	0	0	0	0	0	0	0	0	0	0	0	0	0	0	0	0	0	0	0	0	0	0
G010	1	1	1	1	1	1	1	1	1	1	1	1	1	1	1	1	1	1	1	1	1	1	1	1
G012	1	1	1	1	1	1	1	1	1	1	1	1	1	1	1	1	1	1	1	1	1	1	1	1
G018	0	0	0	0	0	0	0	1	1	1	1	1	1	1	1	1	1	1	1	1	1	1	1	1
G019	0	0	0	0	0	0	0	0	0	1	0	0	0	0	1	0	0	0	0	0	0	0	0	0
G024	0	0	0	0	0	0	0	0	0	0	0	0	0	0	0	0	0	0	0	0	0	0	0	0
G025	1	1	1	1	1	1	1	1	1	1	1	1	1	1	1	1	1	1	1	1	1	1	1	1
G026	1	1	1	1	1	1	1	1	1	1	1	1	1	1	1	1	1	1	1	1	1	1	1	1
G027	0	0	0	0	0	0	0	0	0	0	0	0	0	0	0	0	0	0	0	0	0	0	0	0
G031	0	0	0	0	0	0	0	0	1	1	1	0	0	0	0	0	0	0	0	0	0	0	0	0
G032	0	0	0	0	0	0	0	1	1	1	1	1	1	1	1	1	1	1	1	1	1	1	0	0
G034	0	0	0	0	0	0	0	0	0	1	1	0	0	0	0	0	0	0	0	0	0	0	0	0
G036	0	0	0	0	0	0	0	1	1	1	1	1	1	1	1	1	1	1	1	1	1	1	1	1
G040	0	0	0	0	0	0	0	0	0	0	0	0	0	0	0	0	0	0	0	0	0	0	0	0
G042	0	0	0	0	0	0	0	0	0	1	1	0	0	0	0	0	0	0	0	0	0	0	0	0
G046	0	0	0	0	0	0	0	0	1	1	1	1	1	1	1	1	1	1	0	0	0	0	0	0
G049	1	1	1	1	1	1	1	1	1	1	1	1	1	1	1	1	1	1	1	1	1	1	1	1
G054	0	0	0	0	0	0	1	1	1	1	1	1	1	1	1	1	1	1	1	1	1	1	1	1
G055	0	0	0	0	0	0	0	0	1	1	1	1	1	1	1	1	1	1	1	1	1	1	0	0
G059	0	0	0	0	0	0	0	1	1	1	1	1	1	1	1	1	1	1	1	1	1	1	1	1
G061	0	0	0	0	0	0	0	0	1	1	1	1	1	1	1	1	1	1	1	1	1	1	1	1
G065	1	1	1	1	1	1	1	1	1	1	1	1	1	1	1	1	1	1	1	1	1	1	1	1
G066	1	1	1	1	1	1	1	1	1	1	1	1	1	1	1	1	1	1	1	1	1	1	1	1
G069	1	1	1	1	1	1	1	1	1	1	1	1	1	1	1	1	1	1	1	1	1	1	1	1
G070	1	1	1	1	1	1	1	1	1	1	1	1	1	1	1	1	1	1	1	1	1	1	1	1
G076	1	1	1	1	1	1	1	1	1	1	1	1	1	1	1	1	1	1	1	1	1	1	1	1
G077	1	1	1	1	1	1	1	1	1	1	1	1	1	1	1	1	1	1	1	1	1	1	1	1
G080	1	1	1	1	1	1	1	1	1	1	1	1	1	1	1	1	1	1	1	1	1	1	1	1
G082	0	0	0	0	0	0	1	1	1	1	1	1	1	1	1	1	1	1	1	1	1	1	1	1
G087	0	0	0	0	0	0	0	0	0	0	0	1	1	1	1	1	1	1	1	1	1	1	1	0
G089	1	1	1	1	1	1	1	1	1	1	1	1	1	1	1	1	1	1	1	1	1	1	1	1
G090	0	0	0	0	0	0	0	0	0	0	0	0	0	0	0	0	0	0	0	0	0	0	0	0
G091	0	0	0	0	0	0	0	0	0	0	1	0	0	0	1	0	0	0	0	0	0	0	0	0
G092	1	1	1	1	1	1	1	1	1	1	1	1	1	1	1	1	1	1	1	1	1	1	1	1
G099	0	0	0	0	0	0	0	0	0	0	0	0	0	0	0	0	0	0	0	0	0	0	0	0
G100	1	1	1	1	1	1	1	1	1	1	1	1	1	1	1	1	1	1	1	1	1	1	1	1
G104	0	0	0	0	0	0	0	0	0	1	1	1	1	1	1	1	0	0	0	0	0	0	0	0
G105	0	0	0	0	0	0	0	1	1	1	1	1	1	1	1	1	1	1	1	1	1	1	0	0
G111	0	0	0	0	0	0	0	0	1	1	1	1	1	1	0	0	0	0	0	0	0	0	0	0
G112	0	0	0	0	0	0	0	0	0	0	1	1	1	1	1	1	1	1	1	1	1	1	1	0
G113	1	1	1	1	1	1	1	1	1	1	1	1	1	1	1	1	1	1	1	1	1	1	1	1
G116	0	0	0	0	0	0	0	0	1	1	1	1	1	1	1	1	1	1	1	1	1	1	1	1

Fig. 4 *Unit schedule using NCUC and SCBUC models*

Table 2 Average coherency with respect to COI

Gen number	High load (T12) average correlation	Low load (T5) average correlation
Group 1		
G10	0.892	0.907
G12	0.908	0.929
G25	0.820	0.847
G26	0.886	0.891
G113	0.850	0.884
Group 2		
G49	0.875	0.896
G65	0.916	0.935
G66	0.921	0.943
G70	0.888	0.903
G76	0.826	0.887
G77	0.834	0.881
Group 3		
G80	0.744	0.875
G89	0.893	0.911
G92	0.896	0.957
G100	0.656	0.961

Table 3 Objective costs for different pairs of weighting coefficients

ρ_1	ρ_2	F_1, \$	F_2, *pu*	NCF_1	NCF_2
100	0	861,701.150	414.6765	0	0.1869118
95	5	862,420.856	363.5875	0.0005307	0.1246108
90	10	863,065.730	347.5910	0.0010063	0.1051037
85	15	867,304.622	328.7090	0.0041324	0.0820778
80	20	872,525.55	314.7965	0.0079825	0.065112
75	25	874,156.704	313.0650	0.0091857	0.063001
70	30	875,474.169	306.7200	0.0101572	0.0552631
65	35	879,574.45	301.6575	0.0131812	0.0490896
60	40	881,446.3	301.1390	0.0145616	0.0484573
55	45	881,765.165	301.0840	0.0147967	0.0483902
50	50	882,635.84	299.8665	0.0154388	0.0469055
45	55	885,137.738	299.6945	0.0172839	0.0466958
40	60	887,410.475	299.1800	0.01896	0.0460684
35	65	887,813.881	283.1880	0.019257	0.0265668
30	70	892,080.485	282.6620	0.022404	0.0259253
25	75	896,615.744	270.2215	0.0257487	0.0107546
20	80	897,421.379	269.3475	0.0263428	0.0096888
15	85	899,633.369	269.2265	0.0279742	0.0095413
10	90	904,130.55	269.0585	0.031291	0.009336
5	95	920,171.332	269.0280	0.0431204	0.00929
0	100	925,189.246	261.4023	0.0468211	0

Table 4 Daily costs of NCUC and SCBUC models

Model	Objective function (z)
NCUC	F_1 is optimised and F_2 is just calculated $\left(z = 1 \times \frac{F_1 - F_1^{\min}}{F_1^{\max} - F_1^{\min}} + 0 \times \frac{F_2 - F_2^{\min}}{F_2^{\max} - F_2^{\min}}\right)$ $Z = 0$
SCBUC	F_1 and $F_2$are simultaneously optimised $\left(z = 0.5 \times \frac{F_1 - F_1^{\min}}{F_1^{\max} - F_1^{\min}} + 0.5 \times \frac{F_2 - F_2^{\min}}{F_2^{\max} - F_2^{\min}}\right)$ $Z = 0.03117215$

Model	F_1, \$	F_2, pu
NCUC	861,701.150	414.6765
SCBUC	881,765.165	299.6945

Table 5 Hourly operational and coherency costs using NCUC and SCBUC models

	Model	Time, h							
		T1	T2	T3	T4	T5	T6	T7	T8
operational cost F_1, \$	NCUC	27,294.79	24,479.29	23,736.88	23,908.1	22,842.87	24,935.81	26,767.73	32,596.88
	SCBUC	27,451.54	24,521.45	23,823.39	23,922.85	22,865.42	24,997.64	26,889.66	32,875.18
coherency cost F_2, pu	NCUC	4.74	4.74	4.74	4.74	4.74	4.74	7.30	11.37
	SCBUC	2.25	2.25	2.25	2.25	2.25	2.25	4.70	8.57

	Model	Time, h							
		T9	T10	T11	T12	T13	T14	T15	T16
operational cost F_1, \$	NCUC	38,153.07	42,327.34	44,501.69	44,501.74	43,696.59	44,175.82	44,683.97	42,845.43
	SCBUC	39,265.01	43,195.93	45,140.96	45,239.43	44,705.71	45,042.21	45,422.22	43,988.11
coherency cost F_2, pu	NCUC	21.92	26.30	31.36	25.20	26.83	25.24	26.30	23.89
	SCBUC	15.00	20.79	26.22	20.32	19.15	19.15	21.07	17.25

0.82256 to 0.891326. The average coherency indices, which are calculated by applying short-circuit faults on all lines in four different hours are presented in Table 7. On the basis of Table 7, the coherency of units in SCBUC model is significantly improved compared with the NCUC model.

5.2 Transient stability improvement

Slow coherency positively affects the transient stability of committed synchronous generators. A more coherent group of generators acts as a stronger equivalent generator in COI reference of that group. In this paper, the weighting factors of multi-objective function are determined to reach a minimum CCT. the weighting factors are changed based on the iterative process described in Section 4 from $(\rho_1, \rho_2) = (1, 0)$, i.e. no coherency, in the step of

	Model	Time, h							
		T17	T18	T19	T20	T21	T22	T23	T24
operational cost F_1, $	NCUC	42,236.58	42,205.11	40,892.55	40,130.64	39,658.33	40,993.40	37,525.04	29,943.91
	SCBUC	43,454.62	43,225.28	41,771.54	41,069.38	40,535.56	41,920.25	39,078.35	31,363.45
coherency cost F_2, pu	NCUC	22.83	22.77	21.07	21.13	21.09	21.09	15.90	14.64
	SCBUC	15.95	15.95	15.32	14.81	14.81	14.81	11.52	10.77

Table 6 Comparison of unit scheduling using NCUC and SCBUC and their electrical distance from representative generator

Time		Units going from on to off state and their distance from the representative unit						Units going from off to on state and their distance from the representative unit					
T5	gen number	G070	G076	G077	G113	—	—	G082	G111	G116	—	—	—
	distance, pu	0.3265	0.47375	0.47375	0.3395	—	—	0.16425	0.1976	0.18125	—	—	—
T8	gen number	G018	G032	G036	G076	G077	G105	G004	G031	G040	G042	G061	G090
		G113	—	—	—	—	—	G111	G112	G116	—	—	—
	distance, pu	0.598	0.526375	0.60475	0.47375	0.47375	0.5033	0.278	0.2695	0.228625	0.22625	0.281875	0.2648
		0.339	—	—	—	—	—	0.19775	0.20675	0.1814	—	—	—
T10	gen number	G018	G019	G032	G034	G036	G046	G004	G024	G027	G090	G091	G099
		G055	G076	G077	G104	G105	—	G112	G040	—	—	—	—
	distance, pu	0.598	0.764225	0.52625	0.9008	0.60475	0.555	0.278	0.284575	0.27975	0.26475	0.512	0.25325
		0.5425	0.473775	0.47375	0.5033	0.5035	—	0.256825	0.225775	—	—	—	—
T12	gen number	G018	G032	G036	G046	G055	G076	G004	G027	G031	G040	G042	G090
		G077	G087	G104	G105	—	—	G099	—	—	—	—	—
	distance, pu	0.598	0.526375	0.60475	0.555125	0.5425	0.4737	0.278	0.27975	0.269425	0.2286	0.226175	0.2648
		0.47375	0.477575	0.50325	0.503375	—	—	0.25325	—	—	—	—	—
T15	gen number	G018	G019	G032	G036	G046	G055	G004	G031	G040	G042	G090	G099
		G076	G077	G087	G091	G104	G105	G111	—	—	—	—	—
	distance, pu	0.598	0.764225	0.52625	0.604825	0.55525	0.5426	0.278	0.26925	0.228625	0.226175	0.2648	0.253275
		0.47375	0.4737	0.4775	0.512075	0.50325	0.5034	0.1975	—	—	—	—	—
T19	gen number	G018	G032	G036	G046	G055	G076	G031	G040	G042	G099	G111	—
		G077	G087	G105	G113	—	—	—	—	—	—	—	—
	distance, pu	0.598	0.526375	0.60475	0.555125	0.54275	0.473	0.2695	0.2285	0.226175	0.253275	0.197575	—
		0.47375	0.477575	0.5035	0.338975	—	—	—	—	—	—	—	—

0.05 up to the point at which the transient stability margin of CCT = 100 ms is obtained. In Table 8, the minimum CCT values are reported on a peak load hour (i.e. T12) and a sample light load hour (i.e. T5) for some weighting coefficients.

Note that the CCT calculation is not a part of the optimisation model. Alternatively, by decreasing the electrical distance between committed generators and their related representative generator, as the representative of COI of each group, the coherency and in turn the transient stability is improved. This goal (i.e. providing a minimum CCT of 100 ms) is achieved at $(\rho_1, \rho_2) = (0.5, 0.5)$.

According to Table 8, it can be seen that the minimum CCT of the network has been improved from 0.052 s at T5 and 0.061 s at T12 to 0.101 s at T5 and 0.122 s at T12.

Indeed, the additional cost related to the coherency (i.e. $20,064.015 as obtained in SCBUC model) is indirectly interpreted as the cost of providing a transient stability margin of CCT = 100 ms. The detailed CCT values for all generators at light load (T5) and peak load (T12) have been reported in Table 9. It can be seen that the proposed slow coherency constrained UC model has improved the minimum CCTs, beyond the threshold of 100 ms. The bold values show the cases that the CCT is not acceptable using the NCUC model, while it has been improved using the proposed SCBUC model.

The TSC UC models need high computational burden to give a stable daily unit scheduling plan. However, the proposed method of this paper improves the transient stability, indirectly, based on the slow coherency concept, using a decomposed structure. The steady-state MIP model of the proposed method is solved in the first stage, and in the second stage a dynamic assessment is done to assess the transient stability of the system. The computational time of the first stage, using CPLEX in GAMS, is below 1 s, while the transient stability assessment needs more time to be carried out. A 5 s transient stability assessment is done to assess the transient stability of the unit scheduling plan obtained using MIP model.

6 Conclusion

In this paper, an MILP model was proposed for considering the slow coherency constraint in daily unit scheduling. The stopping criterion for coherency improvement is to reach a minimum value of CCT as the transient stability margin. The major findings of this paper are summarised as follows. (i) direct integration of transient stability criterion in NCUC model is very challenging in both the globality of the commitment schedule and the computational burden. (ii) Using the proposed two-step SCBUC, it was shown that the transient stability may be improved indirectly by promoting the slow coherency via the concept of electrical distance. (iii) According to the obtained results, neglecting the coherency constraint can lead to the commitment of the poorly coherent generators. However, by slightly increasing the total cost of generation, the schedule of units can be modified to improve the transient stability, indirectly. (iv) The simulation results showed that the proposed approach can considerably improve the transient stability of daily unit scheduling by increasing the coherency of generators. The weighting factors of the multi-objective function may be selected accurately through the iterative-based process to provide a minimum value of CCT as the transient stability margin. (v) To reduce the computational complexity, the proposed model can be limited to the period that there is a major risk of transient instability. Although a full coherent commitment schedule may be ideal, however, the operator may select the desired value of

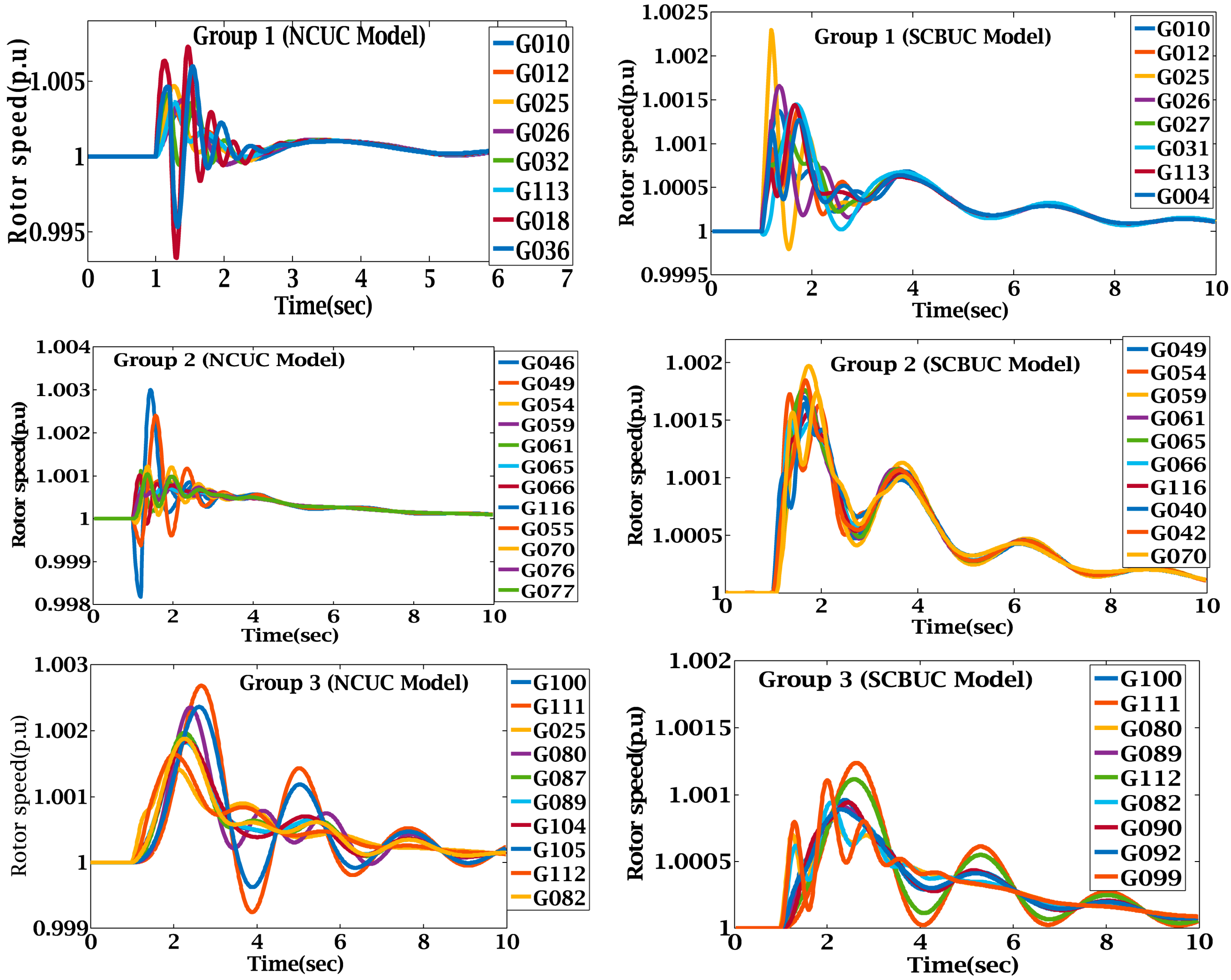

Fig. 5 *Comparison of generators' speeds with and without considering coherency constraint*

Table 7 Comparison of average coherency indices in different hours

Group number	Time, h	
	SCBUC model average correlation	NCUC model average correlation
	T5	
group 1	0.985	0.926
group 2	0.956	0.850
group 3	0.899	0.768
	T8	
group 1	0.910	0.895
group 2	0.930	0.813
group 3	0.855	0.732
	T12	
group 1	0.957	0.936
group 2	0.932	0.850
group 3	0.887	0.730
	T8	
group 1	0.961	0.935
group 2	0.942	0.856
group 3	0.884	0.822

Table 8 CCT results for different weighting factors

Time, h	Minimum CCT, s (ρ_1, ρ_2)					
	(1, 0)	(0.9, 0.1)	(0.7, 0.3)	(0.8, 0.2)	(0.6, 0.4)	(0.5, 0.5)
T5	0.052	0.052	0.068	0.079	0.095	0.101
T12	0.061	0.073	0.087	0.909	0.117	0.122

Table 9 CCT values for different machines assuming $(\rho_1, \rho_2) = (0.5, 0.5)$

Fault Location	CCT			
	NCUC		SCBUC	
	T5	T12	T5	T12
B4	—	—	—	0.521
B10	0.305	0.162	0.421	0.275
B12	0.580	0.175	0.566	0.312
B18	—	0.162	—	—
B25	0.342	0.214	0.368	0.256
B26	0.421	0.228	0.415	0.274
B27	—	—	—	0.697
B31	—	—	—	1.781
B32	—	0.557	—	—
B36	—	0.356	—	—
B40	—	—	—	0.874
B42	—	—	—	1.312
B46	—	0.168	—	—
B49	**0.078**	0.215	**0.11**	0.235
B54	—	0.42	—	0.42
B55	—	0.254	—	—
B59	—	0.619	—	0.461
B61	—	0.415	—	0.354
B65	**0.083**	0.447	**0.123**	0.306
B66	**0.09**	0.485	**0.126**	0.324
B70	**0.052**	0.378	**0.101**	0.914
B76	**0.081**	0.227	—	—
B77	**0.081**	0.181	—	—
B80	**0.082**	0.121	**0.118**	0.213
B82	—	0.265	0.521	0.465
B87	—	**0.061**	—	—
B89	0.377	**0.061**	0.315	0.315
B90	—	—	—	0.974
B92	**0.074**	**0.081**	**0.232**	**0.526**
B99	—	—	—	0.329
B100	**0.086**	0.187	**0.25**	0.338
B104	—	0.726	—	—
B105	—	0.426	—	—
B111	—	0.812	1.125	0.725
B112	—	1.064	—	0.78
B113	0.942	0.699	—	0.491
B116	—	0.221	0.161	0.122

coherency by its willingness to pay the additional cost for transient stability improvement. Future works can investigate the effects of this improvement on small signal stability of the power system.

7 References

[1] Fu, Y., Shahidehpour, M., Li, Z.: 'Security-constrained unit commitment with AC constraints', *IEEE Trans. Power Syst.*, 2005, **20**, (3), pp. 1538–1550

[2] Castillo, A., Laird, C., Silva-Monroy, C.A., *et al.*: 'The unit commitment problem with AC optimal power flow constraints', *IEEE Trans. Power Syst.*, 2016, **31**, (6), pp. 4853–4866

[3] Zárate-Miñano, R., Van Cutsem, T., Milano, F., *et al.*: 'Securing transient stability using time-domain simulations within an optimal power flow', *IEEE Trans. Power Syst.*, 2010, **25**, (1), pp. 243–253

[4] Xu, Y., Dong, Z.Y., Meng, K., *et al.*: 'A hybrid method for transient stability-constrained optimal power flow computation', *IEEE Trans. Power Syst.*, 2012, **27**, (4), pp. 1769–1777

[5] Sun, Y.-Z., Xinlin, Y., Wang, H.F.: 'Approach for optimal power flow with transient stability constraints', *IEE Proc., Gener. Transm. Distrib.*, 2004, **151**, (1), pp. 8–18

[6] Jiang, Q., Huang, Z.: 'An enhanced numerical discretization method for transient stability constrained optimal power flow', *IEEE Trans. Power Syst.*, 2010, **25**, (4), pp. 1790–1797

[7] Xu, Y., Dong, Z.Y., Zhang, R., *et al.*: 'A decomposition-based practical approach to transient stability-constrained unit commitment', *IEEE Trans. Power Syst.*, 2015, **30**, (3), pp. 1455–1464

[8] Jiang, Q., Zhou, B., Zhang, M.: 'Parallel augment Lagrangian relaxation method for transient stability constrained unit commitment', *IEEE Trans. Power Syst.*, 2013, **28**, (2), pp. 1140–1148

[9] Wang, C., Fu, Y.: 'Fully parallel stochastic security-constrained unit commitment', *IEEE Trans. Power Syst.*, 2016, **31**, (5), pp. 3561–3571

[10] Ahmadi, H., Ghasemi, H.: 'Security-constrained unit commitment with linearized system frequency limit constraints', *IEEE Trans. Power Syst.*, 2014, **29**, (4), pp. 1536–1545

[11] Restrepo, J.F., Galiana, F.D.: 'Unit commitment with primary frequency regulation constraints', *IEEE Trans. Power Syst.*, 2005, **20**, (4), pp. 1836–1842

[12] Teng, F., Trovato, V., Strbac, G.: 'Stochastic scheduling with inertia-dependent fast frequency response requirements', *IEEE Trans. Power Syst.*, 2016, **31**, (2), pp. 1557–1566

[13] Khalil, A.M., Iravani, R.: 'A dynamic coherency identification method based on frequency deviation signals', *IEEE Trans. Power Syst.*, 2016, **31**, (3), pp. 1779–1787

[14] Wu, D., Lin, C., Perumalla, V., *et al.*: 'Impact of grid structure on dynamics of interconnected generators', *IEEE Trans. Power Syst.*, 2014, **29**, (5), pp. 2329–2337

[15] Kundur, P., Balu, N.J., Lauby, M.G.: '*Power system stability and control*', vol. **7**, (McGraw-Hill, New York, 1994)

[16] Yang, B., Vittal, V., Heydt, G.T.: 'Slow-coherency-based controlled islanding; a demonstration of the approach on the August 14, 2003 blackout scenario', *IEEE Trans. Power Syst.*, 2006, **21**, (4), pp. 1840–1847

[17] Carrion, M., Arroyo, J.M.: 'A computationally efficient mixed-integer linear formulation for the thermal unit commitment problem', *IEEE Trans. Power Syst.*, 2006, **21**, (3), pp. 1371–1378

[18] Ostrowski, J., Anjos, M.F., Vannelli, A.: 'Tight mixed integer linear programming formulations for the unit commitment problem', *IEEE Trans. Power Syst.*, 2012, **27**, (1), pp. 39–46

[19] Zhang, H., Heydt, G.T., Vittal, V., *et al.*: 'An improved network model for transmission expansion planning considering reactive power and network losses', *IEEE Trans. Power Syst.*, 2013, **28**, (3), pp. 3471–3479
[20] Taylor, J.A., Halpin, S.M.: 'Approximation of generator coherency based on synchronization coefficients'. 2007 39th Southeastern Symp. System Theory, Macon, GA, 2007, pp. 47–51
[21] Taylor, J.A., Sayler, K.A., Halpin, S.M.: 'Approximate prediction of generator dynamic coupling using load flow data'. 2006 38th North American Power Symp., Carbondale, IL, 2006, pp. 289–294
[22] Marler, R.T., Arora, J.S.: 'Survey of multi-objective optimization methods for engineering', *Struct. Multidiscip. Optim.*, 2004, **26**, (6), pp. 369–395
[23] Available at https://github.com/anyacastillo/ucacopf/blob/master/118_ucacopf.dat. Accessed: 15 January 2018
[24] Available at http://www.kios.ucy.ac.cy/testsystems/index.php/dynamic-ieee-test-systems/ieee-118-bus-modified-test-system. Accessed: 15 January 2018
[25] I. CPLEX: 'ILOG CPLEX homepage 2009'. Available at https://www.ibm.com/products/ilog-cplex-optimization-studio, 2009. Accessed: 15 January 2018
[26] Anderson, P.M., Anderson, P.: '*Power system protection*', vol. **1307**, (McGraw-Hill, New York, 1999)